Mechanism of Aβ(1−40) Fibril-Induced Fluorescence of (*trans*,*trans*)-1-Bromo-2,5-bis(4-hydroxystyryl)benzene (K114)[†]

Harry LeVine, III*

Department of Molecular and Cellular Biochemistry, Chandler School of Medicine and the Center on Aging, University of Kentucky, Lexington, Kentucky 40536-0230

Received June 29, 2005; Revised Manuscript Received October 14, 2005

ABSTRACT: K114, (*trans*,*trans*)-1-bromo-2,5-bis(4-hydroxystyryl)benzene, is a fluorescent Congo Red analogue that binds tightly to amyloid fibrils, but not the monomeric proteins, with a concomitant enhancement in fluorescence. The mechanism for the low aqueous fluorescence and the subsequent enhancement by Aβ(1−40) fibrils was investigated by fluorescence spectroscopy and binding analysis. K114's unusually low buffer fluorescence is due to self-quenching in sedimentable aggregates or micelles which upon interacting with amyloid fibrils undergo an enhancement in fluorescence intensity and shifts in the excitation and emission spectra. These spectral changes are suggestive of a stabilization of the phenolate anion, perhaps by hydrogen bonding, rather than an increase in the microenvironment dielectric constant or dye immobilization. 1,4-Bis(4-aminophenylethenyl)-2-methoxybenzene, which lacks the phenol moiety, and X-34, which contains a stabilized phenol (pK ∼13.4), do not display the phenolate anion fluorescence in the presence of fibrils. The apparent affinity of K114 for fibril binding is 20−30 nM with a stoichiometry of 2.2 mol of K114/mol of Aβ(1−40) monomer. Competition studies indicate that K114 and Congo Red share a site, but K114 does not bind to sites on Aβ(1−40) fibrils for neutral benzothiazole (BTA-1), cationic thioflavin T, or the hydrophobic (*S*)-naproxen and (*R*)-ibuprofen molecules. Comparison of benzothiazole binding stoichiometry which has been suggested to reflect disease-relevant amyloid structures to that of Congo Red analogues which reflect total fibril content may be useful in defining biologically pertinent conformational forms of amyloid.

Congo Red (Chart 1, compound **1**) is a sulfonated bisdiazobenzene that binds to amyloid fibrils of proteins with different primary amino acid sequence but a common secondary/tertiary structure which induces a birefringent metachromatic absorbance shift in the dye (*2*). These changes are a defining feature for characterizing fibrillar structures as amyloid fibrils (*3*). Although the structural basis within the fibrils for this interaction with Congo Red remains to be elucidated, the distinctive reactivity with amyloid structures has spawned a series of structural modifications (*4*−*7*). The Congo Red molecule has been used to design smaller derivatives to inhibit fibril formation. Chemists have sought to increase affinity, remove metabolic and toxicological liabilities, and improve blood−brain barrier permeability to produce in vivo imaging agents (*4*, *8*−*10*). Several series, in particular BSB[1] [(*trans*,*trans*)-1-bromo-2,5-bis(3-hydroxycarbonyl-4-hydroxystyryl)benzene] (compound **4**), stain amyloid plaques in AD brain tissue sections and in β-amyloid precursor protein-expressing transgenic animal model brains (*7*, *11*). The high affinity of these molecules for amyloid plaques compared to surrounding components produces a sharp contrast in staining intensity. Binding of BSB to amyloid fibrils has minimal effects on the fluorescence of the dye. One member of the BSB series of derivatives, (*trans*,*trans*)-1-bromo-2,5-bis(4-hydroxystyryl)benzene (K114, compound **5**), has minimal fluorescence in aqueous buffers but fluoresces brightly in the presence of amyloid fibrils of α-synuclein, Aβ(1−40), and tau. The soluble monomeric forms of these proteins do not elicit this fluorescence, allowing K114 to be used to monitor in vitro amyloid fibril formation by fluorescence emission at 550 nm (*12*). We find that, under the conditions of the assay, a potential mechanism for the change in fluorescence of K114 upon the addition of amyloid fibrils is the dye partitioning between an internally quenched particle or micelle of K114 and dye bound to an amyloid fibril, possibly as a stabilized phenolate anion.

MATERIALS AND METHODS

Dimethyl sulfoxide, dimethylformamide, dimethylacetamide, ethanol, 2-propanol, glycerol, and glycine were obtained from Sigma-Aldrich (St. Louis, MO). Acetonitrile and methanol were from Fisher. Thioflavin T, Congo Red, (*S*)-naproxen, (*R*)-ibuprofen, and buffer salts were obtained from Sigma-Aldrich (St. Louis, MO). BTA-1 was purchased from Calbiochem (La Jolla, CA). Aβ(1−40) was provided by California Peptide Research (Napa, CA) (synthetic, lot SF1041; MC0541) and rPeptide (Athens, GA) (recombinant, lot 6180440H).

Fluorescence Measurements. Fixed wavelength fluorescence measurements were made in black plates (Whatman 7701-2350) on a Biotek Synergy HT plate reader. Back-

[†] Funding was provided by the Sanders−Brown Center on Aging and the Chandler Medical Center of the University of Kentucky.

* Corresponding author. E-mail: hlevine@email.uky.edu. Phone: 859-257-1412 ext 224. Fax: 859-323-2866.

[1] Abbreviations: BSB, (*trans*,*trans*)-1-bromo-2,5-bis(3-hydroxycarbonyl-4-hydroxystyryl)benzene; K114, (*trans*,*trans*)-1-bromo-2,5-bis-(4-hydroxystyryl)benzene; DDNP, 2-(*1*) malononitrile; BTA-1, 2-[4′-(methylamino)phenyl]benzothiazole; DMSO, dimethyl sulfoxide.

10.1021/bi051252l CCC: $30.25
Published on Web 11/10/2005

Chart 1: Congo Red-like Molecules[a]

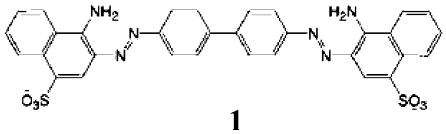

1

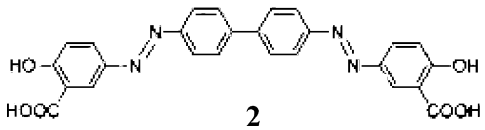

2

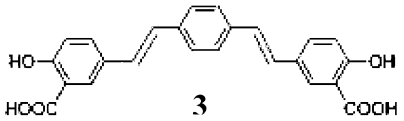

3

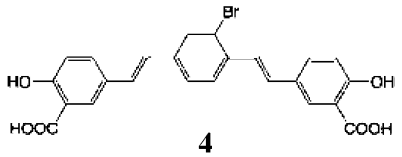

4

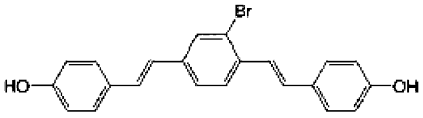

5

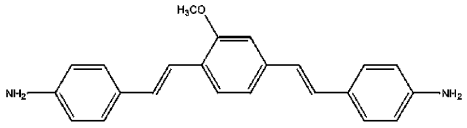

6

Benzothiazoles

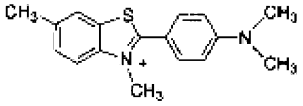

7

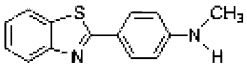

8

[a] Compounds: **1**, Congo Red; **2**, chrysamine G; **3**, X-34; **4**, BSB; **5**, K-114; **6**, 1,4-bis(4-aminophenylethenyl)-2-methoxybenzene; **7**, thioflavin T; **8**, BTA-1.

ground solvent subtracted K114 absorption spectra (background solvent subtracted) and absorbances were determined with the scanning mode of the Synergy HT plate reader in individual wells of clear 96-well plates (Costar 3795) from 400 to 650 nm in 2 nm increments. Fluorescence spectra were obtained on 0.3 mL samples in 1 mL volume, 1 cm path length quartz cuvettes with a Shimadzu RF-5000U spectrofluorometer (150 W xenon lamp) employing 5 and 10 nm excitation and emission slit widths, respectively. Displayed spectra are background solvent, fibril scattering subtracted. Cuvettes were washed with 95% ethanol between samples to remove adsorbed K114 and peptide.

Amyloid Fibril Preparation. Amyloid fibrils were prepared from Aβ(1−40) dissolved at 1 mg/mL in 50 mM sodium phosphate−150 mM NaCl−0.02% NaN_3, pH 7.5, and incubated unstirred at 37 °C for 5 days. Before use the fibrils were sonicated briefly to disperse clumps and washed by centrifugation to remove loosely attached monomer and protofibrils. More than 96% of the peptide and 95% of the amyloid fibril-induced thioflavin T fluorescence were sedimented upon centrifugation at 16000*g* for 15 min. Several different lots of Aβ(1−40) including both synthetic and recombinant peptide were used to make fibrils with similar results.

Measurement of Aβ(1−40) Fibril-Induced K114 Fluorescence. K114 was diluted to the desired concentration from a 100× freshly prepared stock in DMSO. The desired amount of fibrils in 100 mM glycine−NaOH, pH 8.5, was added to the K114 in 200 μL of 100 mM glycine−NaOH, pH 8.5, in wells of a black 96-well plate and mixed. After 5 min the wells were read with a 360/40 nm band-pass excitation and a 530/25 nm band-pass emission filter.

RESULTS

Determination of a Binding Constant and Stoichiometry of K114 for Aβ(1−40) Fibrils. From experiments with radiolabeled BSB derivatives (*12*) the apparent binding affinity for K114 has been projected to be in the 10^{-8} M range. To determine a true affinity, an excess of ligand with respect to the number of binding sites on the fibrils must be provided. A series of concentrations of Aβ(1−40) fibrils were titrated with K114 and the EC_{50}'s determined. A plot of EC_{50} vs fibril concentration was extrapolated to zero fibril concentration, yielding an apparent affinity of 20−30 nM for K114 (Figure 1A,B). An approximate stoichiometry of binding [1 K114 per 2.2 Aβ(1−40) monomers] was determined from the concentration of K114 required for saturation of binding fluorescence at multiple fibril concentrations. This was confirmed by the method of continuous variation (Job analysis) (*13*) ($n = 2.17$), where the mole fraction of fibrils was varied against the mole fraction of K114 (Figure 1C). The symmetry of the Job plot implies that the binding sites on fibrils inducing fluorescence are relatively homogeneous, unlike those for thioflavin T binding (*14*) (*15*) but more like those seen for Congo Red binding.

The insolubility of K114 at micromolar concentrations under conditions of the assay (100 mM glycine−NaOH, pH 8.5) prevented measurement of direct binding of K114 to fibrils by sedimentation (15 kG, 5 min). Addition of cosolvents, which is common in binding assays of this class of compounds (*5*), was avoided because of interfering solvent effects on the dye fluorescence and potential effects on fibril structure. A minimum of 30% ethanol was required to solubilize K114 under these conditions.

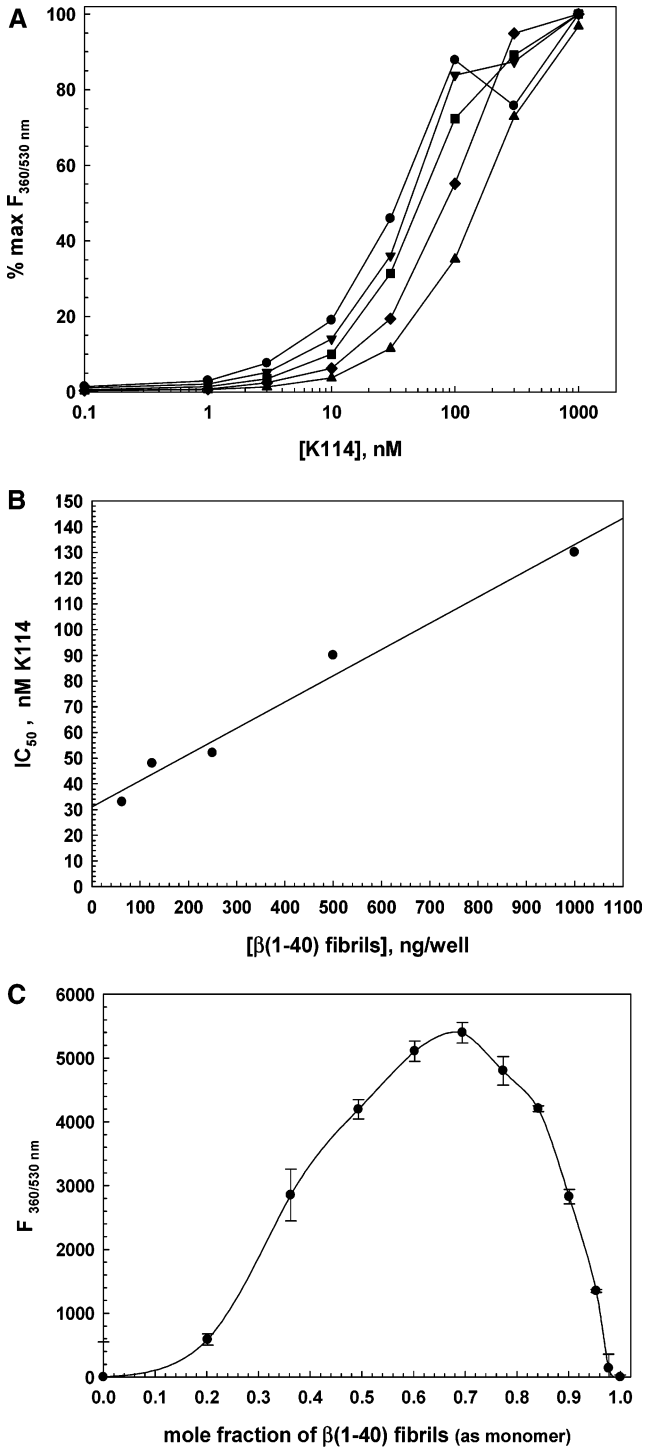

FIGURE 1: K114 binding to Aβ(1−40) fibrils. Panel A: Saturation binding at different Aβ(1−40) fibril concentrations. Increasing concentrations of Aβ(1−40) fibrils were incubated with increasing concentrations of K114 from 0.1 to 1000 nM. Key: (▲) 1000 ng of fibrils/well; (◆) 500 ng/well; (■) 250 ng/well; (▼) 125 ng/well; (●) 62.5 ng/well. Panel B: Extrapolation for determination of the K114 binding constant. Plot of EC_{50}'s determined from panel A extrapolates to 30 nM K114. Panel C: Job plot of K114 stoichiometry for Aβ(1−40) fibrils. A constant total number of moles (150 pmol) of K114 and Aβ(1−40) peptide were co-incubated in 100 mM glycine−NaOH, pH 8.5, at different mole fractions of Aβ(1−40) peptide (expressed as monomer). The peak in a Job plot occurs at a mole fraction of peptide that represents the saturating peptide:K114 ratio [n = 2.17 Aβ(1−40)/K114].

Spectral Properties of K114. The low aqueous solubility of K114 suggested that internal quenching within an insoluble dye droplet or micelle was responsible for the weak aqueous fluorescence of K114. The absorption spectra are in line with this interpretation, exhibiting a pronounced red shift from a maximum at 320 nm to 370 nm with solubilization at high pH, although interpretation is confounded with the electronic effects of the ionization of the phenolic hydroxyls which increase the solubility of the dye. Titration of the phenolic hydroxyls at pH 9.8 (solid line, Figure 2A) corresponded with an enhancement in fluorescence at 530 nm, the solubilizing of K114, and the shift of emission from the 420:450 nm doublet to 520 nm due to the phenolate anion. The titration curve closely follows the solubility of K114 as measured in the supernatant after centrifugation by fluorescence ($F_{360/530\ nm}$) and by absorbance at 360 nm (symbols, Figure 2A).

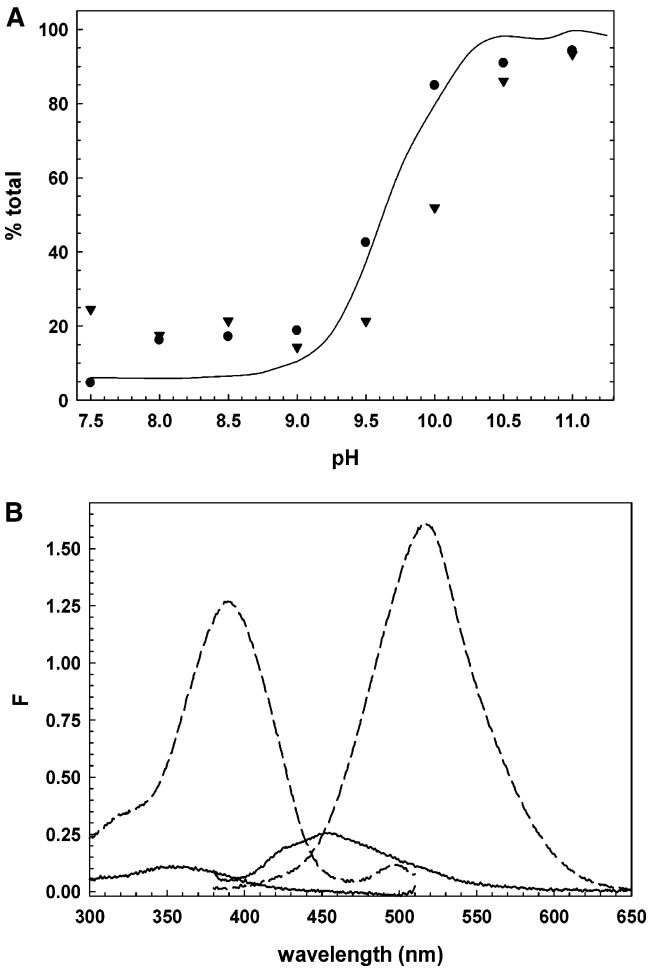

FIGURE 2: pH dependence of K114 fluorescence and solubility. Panel A: Titration of K114 fluorescence. (—) 1 μM K114 was incubated in 0.1 M $NaHCO_3$ buffer at pHs between 7.5 and 11.3 in a black plate in duplicate and the fluorescence measured (360/530 nm) in a plate reader. In a separate experiment 10 μM K114 was incubated at the same pHs and an aliquot centrifuged. The uncentrifuged material and the supernatants were assayed for fluorescence and absorbance of the K114. Key: (●) % soluble by fluorescence at 360/530 nm; (▼) = % soluble by absorbance at 360 nm. Panel B: K114 fluorescence spectra at pH 8.5 and 10.5. Excitation and emission spectra were obtained for 1 μM K114 in 0.1 M $NaHCO_3$ buffer, pH 8.5 (solid line; λ_{ex} = 370 nm, λ_{em} = 450 nm) and pH 10.5 (dashed line; λ_{ex} = 395 nm, λ_{em} = 520 nm).

To determine the effects of stoichiometric ratios of fibrillar β(1−40) on K114 spectral properties and bearing in mind the insolubility of the dye, the concentration of K114 was reduced to 1 μM. The addition of a saturating concentration

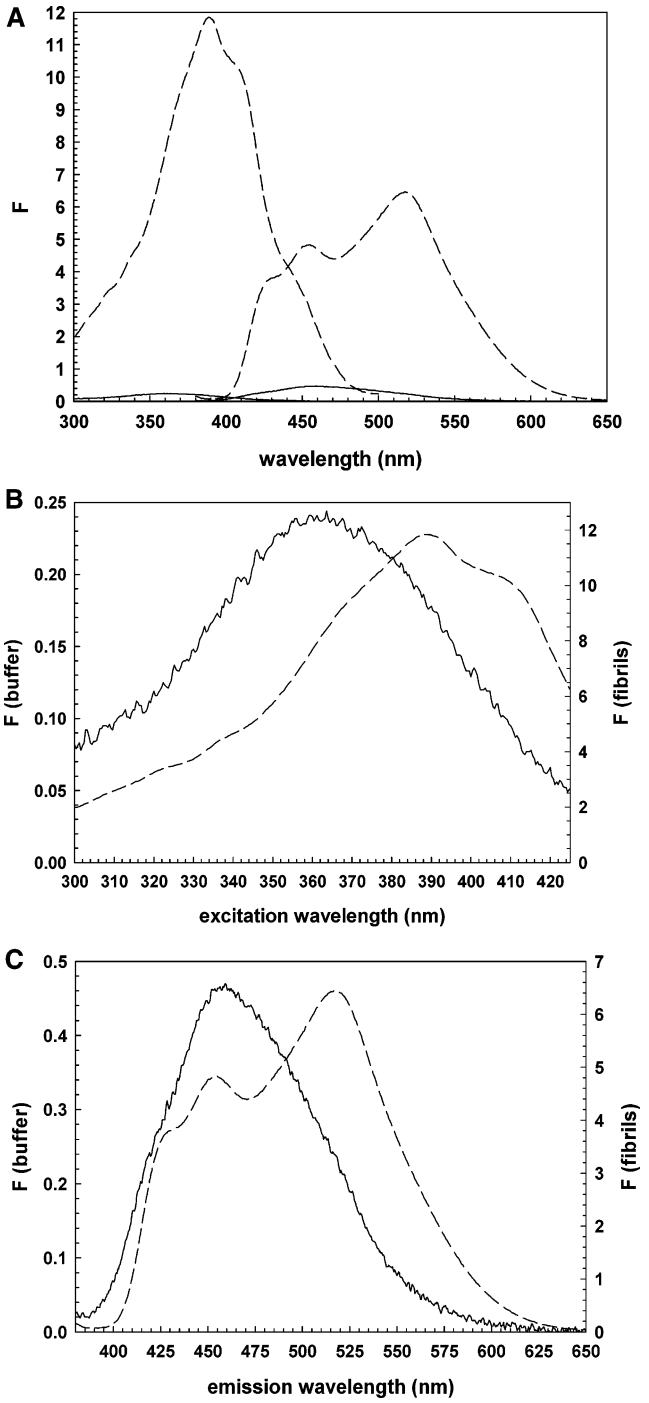

FIGURE 3: Fluorescence spectra of K114 binding to Aβ(1−40) fibrils. Panel A: Spectral changes on binding of K114 to Aβ(1−40) fibrils. Excitation (λ_{em} = 520 nm) and emission spectra (λ_{ex} = 360 nm) were obtained for 1 μM K114 in 0.1 M glycine, pH 8.5, in the absence (solid line) and presence (dashed line) of 3 μM Aβ-(1−40) fibrils (expressed as monomer). Panel B: Expanded excitation spectrum. The excitation spectrum (λ_{em} = 520 nm) in panel A is scaled to equivalent intensities to highlight the spectral shift induced by fibril binding. Spectra are in the absence (solid line) and presence (dashed line) of 3 μM Aβ(1−40) fibrils (expressed as monomer). Panel C: Expanded emission spectrum. The emission spectrum (λ_{ex} = 360 nm) in panel A is scaled to equivalent intensities to highlight the spectral shift induced by fibril binding. Spectra are in the absence (solid line) and presence (dashed line) of 3 μM Aβ(1−40) fibrils (expressed as monomer).

of amyloid fibrils of β(1−40) significantly enhanced the fluorescence of K114 in buffer (Figure 3A), while the equivalent amount of monomeric soluble counterpart did not. Fibril binding induced changes in the wavelength dependence of both the excitation and the emission spectra of K114 as well as a significant enhancement of fluorescence at 450 nm and the appearance of an intense shoulder at 520 nm. The shifts are more readily appreciated in the expanded spectra in Figure 3B,C. In the excitation spectrum (Figure 3B) a peak at 350 nm with unresolved substructure underwent a hypochromic shift and split into partially resolved peaks at 390 nm and at 410 nm. The same emission spectrum was observed for excitation at either 390 or 410 nm, suggesting that the two peaks are not due to sample heterogeneity or scattering artifacts. The emission spectrum (Figure 3C) was essentially that of the free soluble dye with a large shoulder at 520 nm in the position of the phenolate anion emission observed at high pH. The 520 nm emission may be due to microscopic environmental stabilization of the phenolate upon binding to the fibrils.

To test this hypothesis, the spectral characteristics of two styrylbenzene analogues of K114, 1,4-bis(4-aminophenylethenyl)-2-methoxybenzene (compound **6**), which lacks the phenolic OH, and X-34 (compound **3**), which contains a phenolic OH stabilized through intramolecular H-bonding (pK ∼13.4) ortho to a carboxyl, were compared to K114. The methoxybenzene derivative was poorly soluble at pH 8.5, comparable to K114, while X-34 was soluble under these conditions. Figure 4 shows the effect of the addition of a saturating amount of fibrils to the methoxybenzene derivative (panel A) and to X-34 (panel B). In both cases, there is a significant blue shift but no red-shifted 520 nm peak like that seen for K114. At pH 10.5 the fluorescence intensities of the two analogues increased slightly (around 2-fold) but with no shift in the excitation or emission maxima.

The fluorescence intensity enhancement observed when small molecule fluorophores bind to proteins often is the result of a lower dielectric constant in the vicinity of the probe or restriction of molecular motions or solvent relaxation that deactivate the excited state without emission of a photon. Excitation and emission spectra (Figure 5A,B) of K114 solubilized in a series of solvents of different bulk dielectric constant were determined. Solvent polarity was significantly correlated with increasing emission intensity of free K114 at 440 nm (r^2 = 0.94) (Figure 5C) but much less so (r^2 = 0.42) at 520 nm (data not shown). No emission peak or shoulder was observed at 520 nm in the different solvents, suggesting that this emission is a feature of fibril-bound K114. Alterations in wavelengths of emission or excitation were 10 nm or less and not significantly correlated with the dielectric constant. Thus, the fibril-induced excitation spectral shifts and splittings in K114 could not be assigned to changes in the dielectric constant of the probe environment. The enhancement of fluorescence is also not due to removal of a relaxation mechanism by immobilization of a molecular rotor (*16*) as K114 fluorescence is minimally sensitive to viscosity.

K114 Binding Site on β(1−40) Fibrils. Because of their structural similarities, Congo Red was expected to compete with K114 binding. Figure 6 shows the displacement of 1 μM K114 from 0.28 μM β(1−40) fibrils (expressed as monomer) by Congo Red with an apparent IC_{50} of around 70 nM. There is a weak effect of Congo Red on K114 aqueous fluorescence as there is spectral overlap between K114 and Congo Red which may be partially due to

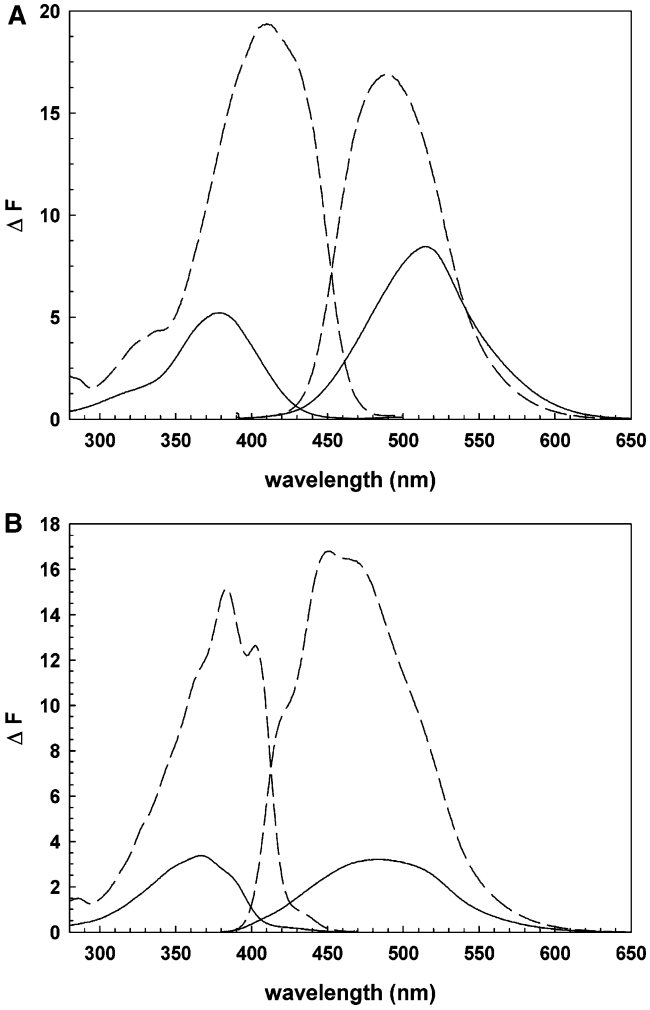

FIGURE 4: Fluorescence spectra of 1,4-bis(4-aminophenylethenyl)-2-methoxybenzene and X-34 binding to Aβ(1−40) fibrils. Panel A: Spectral changes on binding of 1,4-bis(4-aminophenylethenyl)-2-methoxybenzene to Aβ(1−40) fibrils. Excitation (λ_{em} = 515 nm) and emission spectra (λ_{ex} = 380 nm) were obtained for 1.6 μM 1,4-bis(4-aminophenylethenyl)-2-methoxybenzene in 0.1 M glycine, pH 8.5, in the absence (solid line) and presence (dashed line) of 3.2 μM Aβ(1−40) fibrils (expressed as monomer). Panel B: Spectral changes on binding of X-34 to Aβ(1−40) fibrils. Excitation (λ_{em} = 480 nm) and emission spectra (λ_{ex} = 365 nm) were obtained for 1.6 μM X-34 in 0.1 M glycine, pH 8.5, in the absence (solid line) and presence (dashed line) of 3.2 μM Aβ(1−40) fibrils (expressed as monomer).

comicelles. Congo Red could also quench K114 fluorescence if both are bound to fibrils in close proximity which could mimic displacement. By comparison, thioflavin T (compound **7**), BTA-1 (compound **8**, an uncharged thioflavin T derivative), and (*S*)-naproxen and (*R*)-ibuprofen, both of which bind to a site on amyloid fibrils for hydrophobic ligands such as DDNP (*17*), have little effect up to 50 μM against 1 μM K114.

DISCUSSION

K114 is the only molecule reported to change its fluorescence upon binding to amyloid fibrils out of a series of styrylbenzenes modeled on Congo Red (compound **1**), chrysamine G (compound **2**) (*4*), and X-34 (compound **3**) (*18*), including the close analogue BSB [(*trans*,*trans*)-1-bromo-2,5-bis(3-hydroxycarbonyl-4-hydroxystyryl)benzene] (compound **4**). The BSB series is generally highly

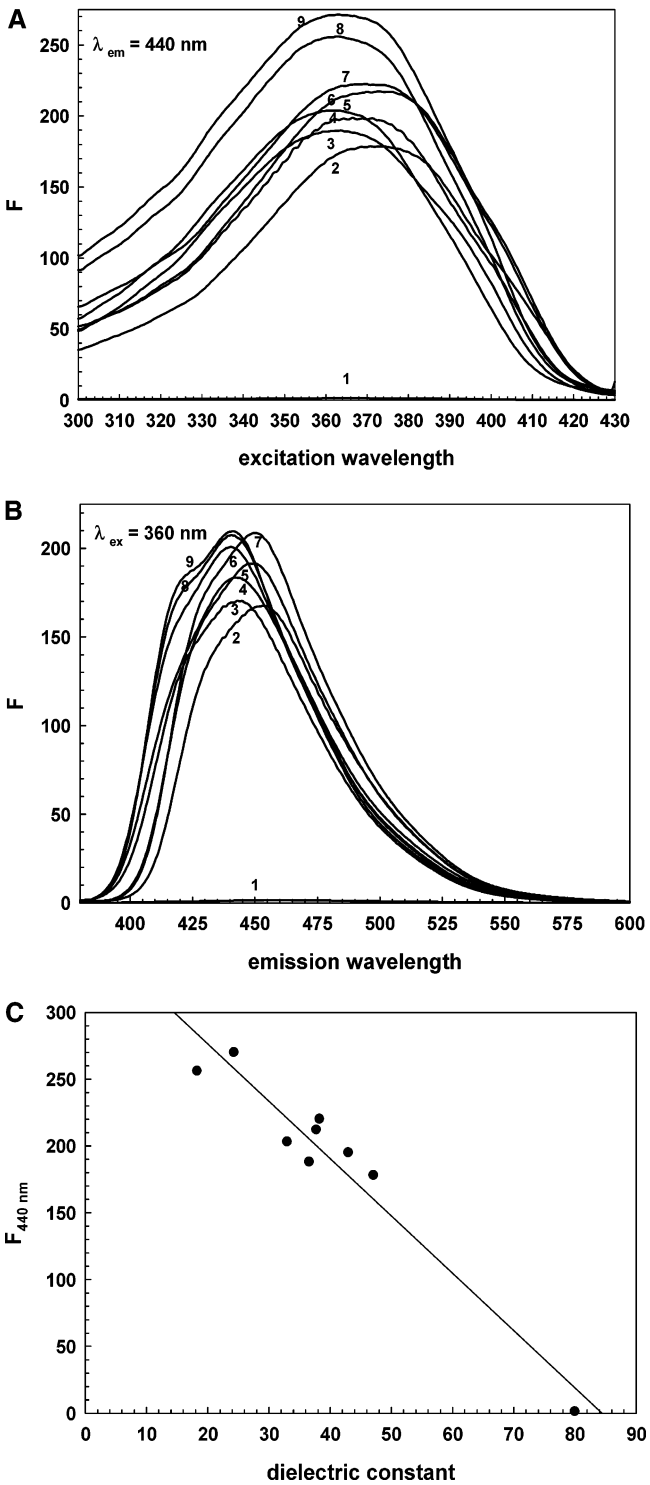

FIGURE 5: Solvent polarity effects on K114 fluorescence. A series of excitation and emission spectra of 10 μM K114 in solvents of different dielectric constant. Key: 1, H_2O; 2, dimethyl sulfoxide; 3, acetonitrile; 4, glycerol; 5, methanol; 6, dimethylacetamide; 7, dimethylformamide; 8, 2-propanol; 9, ethanol. Panel A: Excitation spectra (λ_{em} = 520 nm). Panel B: Emission spectra (λ_{ex} = 360 nm). Panel C: Dielectric constant dependence of K114 fluorescence. Maximum peak fluorescence at 440 nm is plotted against bulk solvent dielectric constant. The line is a linear least-squares fit to the data (r^2 = 0.94).

fluorescent in aqueous solution, associating tightly (~0.1 nM) (*4*), but its properties have not been reported to change upon binding to amyloid. By contrast, K114 (compound **5**) is weakly fluorescent in neutral aqueous buffers. A potential

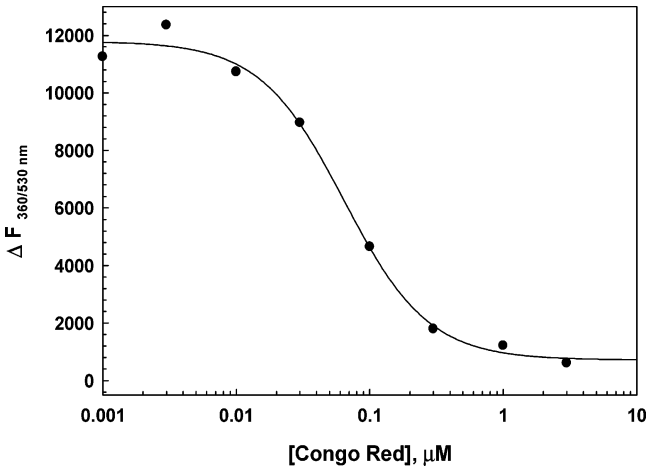

FIGURE 6: Competition of Congo Red for K114 binding to fibrils. 1 μM K114 and 0.28 μM Aβ(1−40) fibrils (expressed as monomer) were titrated with the indicated concentrations of Congo Red. A titration of K114 with Congo Red was performed in the absence of fibrils to adjust for dye−dye interactions.

mechanism for this demonstrated in the present work is that K114 is highly dispersed but sediments at pH 7.5−8.5 in salt-containing buffers (100 mM glycine, pH 8.5; PBS) at 16000*g*. The ionized carboxyl groups on X-34 (compound **3**) increase its solubility so that dilute aqueous solutions are highly fluorescent (Figure 4B). Aggregates of dye molecules, which may be in micelles, experience nonradiative deactivation of the excited state through a variety of mechanisms including exciton coupling, excimer formation, and energy migration to impurity traps (*19*). A blue-shifted aqueous absorbance (320 nm from 370 nm; data not shown) seen for aqueous K114 is consistent with H-aggregate formation in these micelles with parallel dye molecule alignment promoting nonradiative energy transfer. Raising the pH of the buffer solution titrates the phenolic hydroxyls, increasing the solubility of K114 as well as changing its fluorescence. The excitation shifts from 350 to 390 nm and the emission collapses from a doublet at 420:450 nm into a single peak at 520 nm at pHs >9.5. By contrast, X-34 spectra are not shifted, and fluorescence is only weakly increased by raising the pH to 10.5 (data not shown). The explanation for this is that the salicylate moiety (*o*-carboxyphenol) forms an intramolecular hydrogen bond between the phenol OH and the carboxylate, raising the p*K* of the phenol to ∼13.4, well above the normal phenol p*K* of ∼10. Similar results are observed for the 1,4-bis(4-aminophenylethenyl)-2-methoxybenzene (compound **6**) which lacks the phenol.

K114 binding to Aβ(1−40) fibrils at pH 8.5 induces spectral changes in both the excitation and emission spectra. The excitation maximum shifts from 350 nm to a doublet at 390:410 nm. Excitation spectra changes are usually interpreted as alterations in the ground state of the fluorophore. The emission spectrum undergoes enhancement of the doublet at 420:450 nm and a new peak appears at 520 nm. Since the emission spectrum does not shift when the 390 and 410 nm peaks are excited, these are not scattering artifacts and are likely due to different dye-binding environments. Emission spectra are interpreted as changes in the excited state. The emission shoulder at 520 nm is interesting in that it may reflect the stabilization of a phenolate anion or H-bonding of K114 with backbone or side chain residues of the fibril producing a partial phenolate species in the excited state emitting at 520 nm.

X-34 and the methoxystyrylbenzene provide support for this interpretation of the effects of fibril binding on K114. Both compounds show blue shifts of their emission spectra, rather than the red shift (to 520 nm) observed with K114. This suggests that the excited states of the analogue fluorophores are in a less polar environment when bound to the fibril than when in solution. Comparison of the fine structure of the short wavelength region of the K114 emission spectrum to X-34 suggests the same effect, but with the additional 520 nm peak of K114 similar to the ionized phenol form (pH 10.5) of K114. This 520 nm peak would not be expected to form in the amino compound (no phenol) or in the salicylate X-34 (raised phenolic p*K*).

The fibril-induced changes are distinct from those elicited by differences in the dielectric microenvironment or mobility of K114. Varying the bulk dielectric constant of the medium with different solvents altered only the intensity of the K114 emission at 440 nm (no peak at 520 nm) while minimally shifting the excitation or emission wavelengths. Exposure of K114 to glycols such as glycerol does not reproduce the fibril-bound characteristics of K114, unlike the situation for thioflavin T (compound **7**) (*20*).

The competition of Congo Red for binding of K114 to Aβ(1−40) fibrils suggests that the two dyes bind to the same or similar sites, a likely possibility since the structures are related. In support of this, the cationic thioflavin T and uncharged benzothiazole thioflavin T analogue BTA-1 (compound **8**) are unaffected by K114 binding and vice versa. A site for hydrophobic compounds such as DDNP (*17*) on Aβ(1−40) fibrils that partially overlaps with a BTA-1 binding site is distinct from the Congo Red/BSB/K114 binding site. Two compounds that bind avidly to that site, (*R*)-ibuprofen and (*S*)-naproxen, are without effect on K114 binding to fibrils. At least three sites for thioflavin T-like molecules have been defined on Aβ(1−40) fibrils (*15*, *21*).

A characteristic of Congo Red and its derivatives is its stoichiometry of binding to amyloid fibrils. While other dye-binding sites are markedly substoichiometric compared to the peptide monomer content for in vitro fibrils, Congo Red and K114 bind 1:1 and 1:2, respectively. Both perpendicular (*5*) and parallel (*22*) binding modes for the dyes with respect to the polypeptide backbone have been proposed to accommodate the stoichiometry and the observation that binding to amyloid fibrils is primary amino acid sequence-independent. Direct structural confirmation of binding modes in Aβ amyloid fibrils is lacking. The binding stoichiometry of benzothiazole ligands has been suggested as reflecting disease-relevant amyloid structures in Alzheimer's disease (*23*). ^{11}C-6-OH-BTA-1 amyloid from AD brain binds 1:1, APP/PS1 transgenic mouse brain 1:100, and synthetic Aβ fibrils 1:370 (ligand:monomer peptide) (*23*−*26*). It is clear from prions (*27*) and Aβ (*28*, *29*) that multiple self-propagating conformational forms or "strains" of amyloid fibrils exist. Comparison of the relative amounts of binding of Congo Red analogues such as BSB derivatives and benzothiazoles may be useful in defining biologically relevant conformational forms of amyloid.

ACKNOWLEDGMENT

The author thanks Dr. Virginia M.-Y. Lee (University of Pennsylvania School of Medicine) for providing the K114 for these experiments. X-34 and 1,4-bis(4-aminophenylethenyl)-2-methoxybenzene were generous gifts from Drs. William B. Klunk and Chester A. Mathis (University of Pittsburgh).

SUPPORTING INFORMATION AVAILABLE

Fluorescence micrographs of AD brain cortex sections stained with K114 or X-34 revealing brightly labeled neuritic plaques. This material is available free of charge via the Internet at http://pubs.acs.org.

REFERENCES

1. Shoghi-Jadid, K., Small, G. W., Agdeppa, E. D., Kepe, V., Ercoli, L. M., Siddarth, P., Read, S., Satyamurthy, N., Petric, A., Huang, S. C., and Barrio, J. R. (2002) Localization of neurofibrillary tangles and beta-amyloid plaques in the brains of living patients with Alzheimer disease, *Am. J. Geriatr. Psychiatry 10*, 24−35.
2. Klunk, W. E., Jacob, R. F., and Mason, R. P. (1999) Quantifying amyloid by congo red spectral shift assay, *Methods Enzymol. 309*, 285−305.
3. Kelenyi, G. (1967) Thioflavin S fluorescent and Congo red anisotropic stainings in the histologic demonstration of amyloid, *Acta Neuropathol. (Berlin) 7*, 336−348.
4. Kung, M. P., Hou, C., Zhuang, Z. P., Skovronsky, D. M., Zhang, B., Gur, T. L., Trojanowski, J. Q., Lee, V. M., and Kung, H. F. (2002) Radioiodinated styrylbenzene derivatives as potential SPECT imaging agents for amyloid plaque detection in Alzheimer's disease, *J. Mol. Neurosci. 19*, 7−10.
5. Klunk, W. E., Debnath, M. L., and Pettegrew, J. W. (1995) Chrysamine-G binding to Alzheimer and control brain: autopsy study of a new amyloid probe, *Neurobiol. Aging 16*, 541−548.
6. Zhuang, Z. P., Kung, M. P., Hou, C., Skovronsky, D. M., Gur, T. L., Plossl, K., Trojanowski, J. Q., Lee, V. M., and Kung, H. F. (2001) Radioiodinated styrylbenzenes and thioflavins as probes for amyloid aggregates, *J. Med. Chem. 44*, 1905−1914.
7. Schmidt, M. L., Schuck, T., Sheridan, S., Kung, M. P., Kung, H., Zhuang, Z. P., Bergeron, C., Lamarche, J. S., Skovronsky, D., Giasson, B. I., Lee, V. M. Y., and Trojanowski, J. Q. (2001) The fluorescent congo red derivative, (*trans*,*trans*)-1-bromo-2,5-bis-(3-hydroxycarbonyl-4-hydroxy)styrylbenzene (BSB), labels diverse beta-pleated sheet structures in postmortem human neurodegenerative disease brains, *Am. J. Pathol. 159*, 937−943.
8. Kung, M. P., Skovronsky, D. M., Hou, C., Zhuang, Z. P., Gur, T. L., Zhang, B., Trojanowski, J. Q., Lee, V. M., and Kung, H. F. (2003) Detection of amyloid plaques by radioligands for Abeta40 and Abeta42: potential imaging agents in Alzheimer's patients, *J. Mol. Neurosci. 20*, 15−24.
9. Ishikawa, K., Doh-ura, K., Kudo, Y., Nishida, N., Murakami-Kubo, I., Ando, Y., Sawada, T., and Iwaki, T. (2004) Amyloid imaging probes are useful for detection of prion plaques and treatment of transmissible spongiform encephalopathies, *J. Gen. Virol. 85*, 1785−1790.
10. Sato, K., Higuchi, M., Iwata, N., Saido, T. C., and Sasamoto, K. (2004) Fluoro-substituted and (13)C-labeled styrylbenzene derivatives for detecting brain amyloid plaques, *Eur. J. Med. Chem. 39*, 573−578.
11. Skovronsky, D. M., Zhang, B., Kung, M. P., Kung, H. F., Trojanowski, J. Q., and Lee, V. M. (2000) In vivo detection of amyloid plaques in a mouse model of Alzheimer's disease, *Proc. Natl. Acad. Sci. U.S.A. 97*, 7609−7614.
12. Crystal, A. S., Giasson, B. I., Crowe, A., Kung, M. P., Zhuang, Z. P., Trojanowski, J. Q., and Lee, V. M. (2003) A comparison of amyloid fibrillogenesis using the novel fluorescent compound K114, *J. Neurochem. 86*, 1359−1368.
13. Huang, C. Y. (1982) Determination of binding stoichiometry by the continuous variation method: the Job plot, *Methods Enzymol. 87*, 509−525.
14. LeVine, H., III (1997) Stopped-flow kinetics reveal multiple phases of thioflavin T binding to Alzheimer beta (1−40) amyloid fibrils, *Arch. Biochem. Biophys. 342*, 306−316.
15. Lockhart, A., Ye, L., Judd, D. B., Merritt, A. T., Lowe, P. N., Morgenstern, J. L., Hong, G., Gee, A. D., and Brown, J. (2005) Evidence for the presence of three distinct binding sites for the thioflavin T class of Alzheimer's disease PET imaging agents on beta-amyloid peptide fibrils, *J. Biol. Chem. 280*, 7677−7684.
16. Haidekker, M. A., Brady, T. P., Chalian, S. H., Akers, W., Lichlyter, D., and Theodorakis, E. A. (2004) Hydrophilic molecular rotor derivatives-synthesis and characterization, *Bioorg. Chem. 32*, 274−289.
17. Agdeppa, E. D., Kepe, V., Petri, A., Satyamurthy, N., Liu, J., Huang, S. C., Small, G. W., Cole, G. M., and Barrio, J. R. (2003) In vitro detection of (S)-naproxen and ibuprofen binding to plaques in the Alzheimer's brain using the positron emission tomography molecular imaging probe 2-(1-[6-[(2-[(18)F]fluoroethyl)(methyl)-amino]-2-naphthyl]ethylidene)malono nitrile, *Neuroscience 117*, 723−730.
18. Styren, S. D., Hamilton, R. L., Styren, G. C., and Klunk, W. E. (2000) X-34, a fluorescent derivative of Congo red: a novel histochemical stain for Alzheimer's disease pathology, *J. Histochem. Cytochem. 48*, 1223−1232.
19. An, B. K., Kwon, S. K., Jung, S. D., and Park, S. Y. (2002) Enhanced emission and its switching in fluorescent organic nanoparticles, *J. Am. Chem. Soc. 124*, 14410−14415.
20. LeVine, H., III (1995) Thioflavine T interaction with amyloid β-sheet structures, *Amyloid: Int. J. Exp. Clin. Invest. 2*, 1−6.
21. LeVine, H., III (2005) Multiple ligand binding sites on A beta-(1−40) fibrils, *Amyloid 12*, 5−14.
22. Carter, D. B., and Chou, K. C. (1998) A model for structure-dependent binding of Congo red to Alzheimer beta-amyloid fibrils, *Neurobiol. Aging 19*, 37−40.
23. Mathis, C. A., Wang, Y., Holt, D. P., Huang, G. F., Debnath, M. L., and Klunk, W. E. (2003) Synthesis and evaluation of 11C-labeled 6-substituted 2-arylbenzothiazoles as amyloid imaging agents, *J. Med. Chem. 46*, 2740−2754.
24. Klunk, W. E., Lopresti, B. J., Debnath, M. L., Holt, D. P., Wang, Y., Huang, G.-F., Shao, L., Lefterov, I., Koldamova, R., Ikonomovic, M., DeKosky, S. T., and Mathis, C. A. (2004) Amyloid deposits in transgenic PS1/APP mice do not bind the amyloid PET tracer, PIB, in the same manner as human brain amyloid, *Neurobiol. Aging 25*, 232.
25. Kung, M. P., Hou, C., Zhuang, Z. P., Skovronsky, D., and Kung, H. F. (2004) Binding of two potential imaging agents targeting amyloid plaques in postmortem brain tissues of patients with Alzheimer's disease, *Brain Res. 1025*, 98−105.
26. Zhuang, Z. P., Kung, M. P., Wilson, A., Lee, C. W., Plossl, K., Hou, C., Holtzman, D. M., and Kung, H. F. (2003) Structure−activity relationship of imidazo[1,2-a]pyridines as ligands for detecting beta-amyloid plaques in the brain, *J. Med. Chem. 46*, 237−243.
27. Tanaka, M., Chien, P., Naber, N., Cooke, R., and Weissman, J. S. (2004) Conformational variations in an infectious protein determine prion strain differences, *Nature 428*, 323−328.
28. O'Nuallain, B., Williams, A. D., Westermark, P., and Wetzel, R. (2004) Seeding specificity in amyloid growth induced by heterologous fibrils, *J. Biol. Chem. 279*, 17490−17499.
29. Petkova, A. T., Leapman, R. D., Guo, Z., Yau, W. M., Mattson, M. P., and Tycko, R. (2005) Self-propagating, molecular-level polymorphism in Alzheimer's beta-amyloid fibrils, *Science 307*, 262−265.

BI051252L